Letter

Thermodynamic ground and Berry-phase origin of the planar spin Hall effect

Haolin Pan,[1,2] Zheng Liu,[1] Dazhi Hou,[1,2,*] Yang Gao,[1,2,3,†] and Qian Niu[1,2,3]

[1]*Department of Physics, University of Science and Technology of China, Hefei, Anhui 230026, China*

[2]*Hefei National Research Center for Physical Sciences at the Microscale, University of Science and Technology of China, Hefei, Anhui 230026, China*

[3]*Hefei National Laboratory, University of Science and Technology of China, Hefei 230088, China*

(Received 4 October 2021; accepted 25 January 2024; published 21 February 2024)

The thermodynamic ground of the spin transport is elaborated, demonstrating the Onsager's reciprocal relation. The latter is also confirmed by deriving the spin Hall effect and its inverse using the semiclassical theory and the linear response theory. Importantly, the intrinsic contribution to the spin conductivity that satisfies the Onsager's relation has only Hall-type component and hence does not dissipate heat, in analogy to the anomalous Hall effect and fulfilling the thermodynamic requirement. Based on the expression of the spin Hall conductivity, the Berry-phase origin is elaborated for the recent-discovered planar spin Hall effect which features current-induced spin polarization within the plane of the Hall deflection. We unravel a spin-repulsion vector governing the planar spin Hall effect, providing a transparent criteria for identifying intrinsic planar spin Hall materials. Finite spin-repulsion vector is found permitted in 13 crystalline point groups, revealing a big number of unexplored planar spin Hall systems. Our result can be used for the quantitative calculation of the planar spin Hall effect, facilitating further material hunting and experimental investigation.

DOI: 10.1103/PhysRevResearch.6.L012034

The spin Hall effect (SHE) generates a pure spin current (j_s) perpendicular to the applied charge current (j_c) with the spin direction (s) orthogonal to both j_s and j_c [1]. Such geometrical configuration confines the SHE-induced spin polarization within the x-y plane for a film sample of z normal direction as illustrated in Fig. 1(a). Recent experiment shows that a spin polarization of the z direction (s_z) can be induced by an in-plane charge current in a material with a mirror plane, e.g., $MoTe_2$, as illustrated in Fig. 2(b), which was termed as the planar spin Hall effect (PSHE) [2]. Such a current-induced s_z, which is out of reach for the spin Hall effect, is highly desirable for device development because it can switch ferromagnetic layer of perpendicular magnetic anisotropy (PMA) without involving structural or magnetic field induced asymmetry [3,4]. Such phenomenon was also found in other low-symmetry materials, although the terminologies adopted for the phenomenon description are different [5–12].

However, only a handful of materials have been identified to host the PSHE, and the only clue, the mirror-plane symmetry [5], still lacks proper microscopic interpretation. To facilitate the material hunting, a microscopic theory of the PSHE is indispensable. The spin conductivity σ_{ijk}, defined as $J_j^{s_i} = \sigma_{ijk}E_k$, is usually interpreted as a full rank-3 pseudotensor [13–23], based on the Kubo formula for the local spin current operator $\hat{J}_j^{s_i} = \frac{1}{2}(\hat{v}_j\hat{s}_i + \hat{s}_i\hat{v}_j)$. However, it is shown that to obtain the transport spin current, additional contribution to $\hat{J}_j^{s_i}$ from spin dynamics is needed [24–27]. Despite several pioneer works towards such direction [24–35], the thermodynamic ground and the geometric origin of the transport spin conductivity similar to that in the anomalous Hall effect is still unclear. Such understanding is tied to the symmetry requirement of the PSHE and can deliver a timing guideline for its further development.

In this Letter, we establish the thermodynamic ground of the spin transport based on the entropy production rate and demonstrate the Onsager's reciprocal relation for the spin Hall effect and its inverse. We then derive the transport spin current from the electric field, as well as the charge current from the spin current injection, to further confirm the Onsager's relation.

The most striking feature is that the intrinsic part of the transport spin conductivity σ_{ijk} is of rank 2, in sharp contrast to the previous knowledge of rank 3. Specifically, $\sigma_{ijk} = -\varepsilon_{jka}D_{ai}$ with D_{ai} the spin-weighted Berry curvature as defined in Eq. (12). The presence of the Levi-Civita symbol ϵ_{jka} dictates that the intrinsic contribution to the spin transport is always of the Hall type, i.e., the spin current always flows perpendicular to the electric field. Such an intrinsic contribution does not dissipate heat, in accordance with the thermodynamic requirement. This is in analogy with the charge transport, whose intrinsic contribution is also purely of the Hall type, i.e., the anomalous Hall effect.

From the rank-2 feature of the intrinsic spin conductivity, the symmetry requirement of the PSHE can be deduced straightforwardly. Interestingly, the PSHE is determined by

*dazhi@ustc.edu.cn
†ygao87@ustc.edu.cn

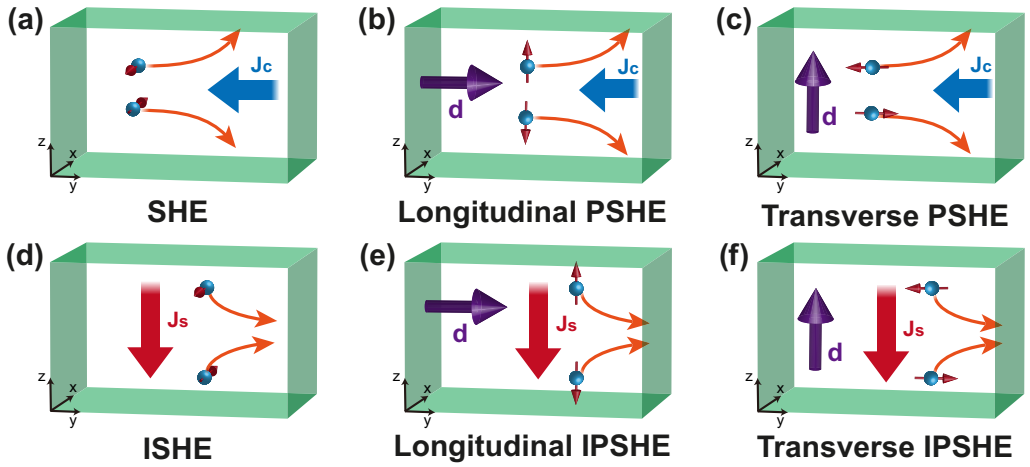

FIG. 1. Geometrical configuration for the conventional (a) and planar (b), (c) spin Hall effect; the conventional (d) and planar (e), (f) inverse spin Hall effect. $\boldsymbol{d}$ is the spin-repulsion vector. Depending on whether $\boldsymbol{d}$ is parallel to the charge or spin flow, we have longitudinal and transverse (inverse) planar spin Hall effect, in which the spin polarization is collinear and perpendicular to the spin current direction, respectively.

a single-spin-repulsion vector $\boldsymbol{d}$, defined from the antisymmetric part of D_{ai} (see Fig. 1). We identify 13 crystalline point groups and 30 magnetic point groups permitting finite $\boldsymbol{d}$ and hence allowing the PSHE. Several existing experiments for PSHE in materials with mirror symmetries can be well subsumed in our theory and we further predict candidate materials with rotational symmetries as potential platforms of the PSHE.

Onsager's reciprocal relation for spin transport. We first establish the thermodynamic ground of the spin transport. The entropy production rate P_S plays a central role in discussing various irreversible processes. It is defined as the part of the changing rate of the entropy that is not carried by the entropy flow [36]:

$$\rho\frac{ds}{dt} = -\nabla\cdot\boldsymbol{J}_S + P_S, \tag{1}$$

where ρ, s, and $\boldsymbol{J}_S$ are the density, entropy per mass, and entropy current, respectively.

To derive P_S, we use the first law of thermodynamics:

$$dU = T\,dS - p\,dV + \mu\;dN, \tag{2}$$

which relates the entropy with other state variables, i.e., the internal energy U, the volume V, the particle number N, with corresponding parameters given by temperature T, pressure p, and chemical potential μ. The internal energy can be obtained from the total energy, calculated by the expectation value of the crystal Hamiltonian $\hat{H}_0$ and the Zeeman potential energy ϕ_Z. Taking the time derivative of Eq. (1), and plugging the result in Eq. (1), we can relate the entropy production rate with the time variation of various state variables.

To further simplify the result, we use the dynamical equation for the spin density, given by [25,26]

$$\frac{\partial\rho_S}{\partial t} = -\nabla\cdot\boldsymbol{J}_S^0 + \boldsymbol{T}, \tag{3}$$

where $\boldsymbol{J}_S^0 = \langle\hat{\boldsymbol{s}}\hat{\boldsymbol{v}}\rangle$ is the local spin current and $\boldsymbol{T} = \langle -i[\hat{\boldsymbol{s}}, \hat{H}]\rangle$ is the spin torque. Equation (3) can be further manipulated to become more suitable for discussing the Onsager's reciprocal relation. Similar to the charge density [37–39], the spin torque also adopts an expansion with respect to spatial variation, originating from the coarse-graining process. The result reads as

$$\boldsymbol{T} = \boldsymbol{T}^f - \nabla\cdot\boldsymbol{P}^T + \cdots, \tag{4}$$

where $\boldsymbol{T}^f$ is the free spin torque, i.e., the part that is uniform within a unit cell, and $\boldsymbol{P}^T = \langle -i[\hat{\boldsymbol{s}}, \hat{H}]\boldsymbol{r}\rangle$ is the dipole of the spin torque.

Combining Eqs. (1) to (4), we obtain the following entropy production rate [40]:

$$P_S = -\frac{\lambda}{T}\boldsymbol{J}_S\cdot\nabla\boldsymbol{B}^Z - \frac{\lambda}{T}\mathcal{T}^f\cdot\boldsymbol{B}^Z, \tag{5}$$

where $\boldsymbol{B}^Z$ is the Zeeman field and $\lambda = g\mu_B/\hbar$ with g and μ_B being the gyromagnetic ratio and the Bohr magneton, respectively, and $\boldsymbol{J}_S = \boldsymbol{J}_S^0 + \boldsymbol{P}^T$. We note that the standard form of the entropy production rate using the generalized force $\boldsymbol{F}$ and current $\boldsymbol{J}$ reads as $\frac{1}{T}\boldsymbol{J}\cdot\boldsymbol{F}$. Equation (5) then suggests that the spin dynamics contributes to two entropy production processes: the force $-\boldsymbol{B}^Z$ drives the procession of the spin magnetization represented by the torque $\lambda\boldsymbol{T}^f$, while the force $-\nabla\boldsymbol{B}^Z$ drives the flow of the spin represented by the spin-magnetization current $\lambda\boldsymbol{J}_S$. The focus of this work is the latter one.

Interestingly, the spin current $\boldsymbol{J}_S$ contains not only the local one $\boldsymbol{J}_S^0$ but also the spin torque dipole $\boldsymbol{P}^T$. In fact, $\boldsymbol{J}_S^0$ and $\boldsymbol{P}^T$ are indistinguishable from the point of view of the entropy production rate. It is thus natural to group them together as the total spin current. By such definition, $\boldsymbol{J}_S$ has a unique property compared with $\boldsymbol{J}_S^0$: it is the time derivative of the spin dipole, i.e., $J_S = d(\boldsymbol{r}\hat{\boldsymbol{s}})/dt$.

We now proceed to prove the Onsager's reciprocal relation for the spin transport. For this purpose, we follow Ref. [41] and assume that near equilibrium the system can be described by a list of state variables $x_1, x_2, \ldots, x_n$. Examples of x_i can be the electric polarization for charge transport, the energy polarization for thermal transport, and the above spin dipole for the spin transport. Since the entropy reaches maximum

at equilibrium, for fluctuation near equilibrium, the entropy should take a parabolic form: $\delta S = -\beta_{ij} x_i x_j$. One can then obtain the entropy production rate: $dS/dt = \sum_i f_i \dot{x}_i$ with $f_i = \partial S/\partial x_i$ being the generalized force and $\dot{x}_i$ being the generalized current. By using the total spin current, the first term in Eq. (5) that is responsible for spin current now has such form. For response coefficients defined as $\dot{x}_i = \gamma_{ij} f_j$, one can then establish the Onsager's reciprocal relation. Specifically, for the spin conductivity defined as $J_i = \sigma_{ijk}\partial_j B_k^Z$ and $J_i^{s_j} = \sigma'_{ijk} E_k$, we have [40]

$$\sigma_{ijk}(\boldsymbol{M}) = -\sigma'_{jki}(-\boldsymbol{M}), \tag{6}$$

where $\boldsymbol{M}$ stands for the magnetic order of the system.

The Onsager's relation is essential in transport theory. It has been shown to hold for the charge and energy current [42]. However, its existence for spin current is previously under debate [17,26]. Here we prove that it holds for the spin transport only when the total spin current is used. We comment that in Ref. [17], Onsager's relation is only objected for the local, but not total, spin current.

Microscopic theory. We now derive the intrinsic contribution to the spin conductivity and show that it fulfills the Onsager's reciprocal relation. To derive the charge current at the order of $\partial_{\boldsymbol{r}} \boldsymbol{B}^Z(\boldsymbol{r})$, we adopt the semiclassical formalism. Under an inhomogeneous $\boldsymbol{B}^Z(\boldsymbol{r})$, the electron motion is governed by the following equations of motion [38]:

$$\dot{\boldsymbol{r}} = \partial_{\boldsymbol{k}} \tilde{\varepsilon}_n - \dot{\boldsymbol{k}} \times \boldsymbol{\Omega}_n - \boldsymbol{\Omega}_{\boldsymbol{kr},n} \cdot \dot{\boldsymbol{r}}, \tag{7}$$

$$\dot{\boldsymbol{k}} = -\partial_{\boldsymbol{r}} \phi + \boldsymbol{\Omega}_{\boldsymbol{rk},n} \cdot \dot{\boldsymbol{k}}, \tag{8}$$

where $\boldsymbol{\Omega}_n = -2\,\mathrm{Im}\langle \partial_{\boldsymbol{k}} n| \times |\partial_{\boldsymbol{k}} n\rangle$ is the momentum-space Berry curvature in band n, $(\boldsymbol{\Omega}_{\boldsymbol{kr},n})_{ij} = -2\,\mathrm{Im}\langle \partial_{k_i} n|\partial_{r_j} n\rangle$ is the mixed Berry curvature with $(\boldsymbol{\Omega}_{\boldsymbol{kr},n})_{ij} = -(\boldsymbol{\Omega}_{\boldsymbol{rk},n})_{ji}$, and $|n\rangle$ is short for $|u_{n\boldsymbol{k}}\rangle$, representing the periodic part of the Bloch wave function. In the velocity equation, $\tilde{\varepsilon}_n$ is the field-corrected nth band energy: $\tilde{\varepsilon}_n = \varepsilon_n + \sum_{ij} \partial_i B_j^Z q_{ij}^S$, where ε_n is the band energy without the Zeeman field, and the remaining term is the magnetic quadrupolar energy [43]. In the force equation, $\phi = -g_S \sum_i \lambda B_i^Z(\boldsymbol{r})\langle n|s_i|n\rangle$ is the Zeeman potential energy, whose gradient offers the driving force for the electron motion. As a result, the electron can only reach equilibrium with $\tilde{\varepsilon}_n$ but not ϕ, leaving the equilibrium Fermi distribution in the form of $f(\tilde{\varepsilon}_n)$.

Another complexity in deriving the transport charge current is that in inhomogeneous systems, the magnetization current generally exists and should be subtracted from the total current, i.e., $J = J_{\mathrm{tot}} - \nabla \times \boldsymbol{M}(\boldsymbol{r})$. In our case, since the magnetic susceptibility is allowed in any material, an inhomogeneous Zeeman field $\boldsymbol{B}^Z(\boldsymbol{r})$ always induces a spatially varying $\boldsymbol{M}(\boldsymbol{r})$. After discounting such magnetization current, the transport current reads as [38]

$$\boldsymbol{J} = -\sum_n \int \frac{d\boldsymbol{k}}{8\pi^3} \mathcal{D} \dot{\boldsymbol{r}} f_n(\tilde{\varepsilon}_n) + \nabla_{\boldsymbol{r}} \times \sum_n \int \frac{d\boldsymbol{k}}{8\pi^3} \boldsymbol{\Omega}_n g_n, \tag{9}$$

where $\mathcal{D} = 1 + \mathrm{Tr}\boldsymbol{\Omega}_{kr,n}$ and $g_n = -k_B T \log\{1 + \exp[(\mu - \varepsilon_n)/k_B T\}$. Since we need the current on the order of $\partial_{\boldsymbol{r}} \boldsymbol{B}^Z$, the Berry curvature $\boldsymbol{\Omega}_n$ should be corrected as follows: $\boldsymbol{\Omega}_n \to \boldsymbol{\Omega}_n + \delta\boldsymbol{\Omega}_n$, where $\delta\boldsymbol{\Omega}_n$ is proportional to $\boldsymbol{B}^Z$. Such correction can be obtained using standard perturbative procedure in the semiclassical formalism.

By plugging all relevant elements into Eq. (9), the final expression of the spin conductivity reads as [40]

$$\sigma_{ijk} = -\epsilon_{iaj} D_{ak}, \tag{10}$$

where D_{ab} is a tensor representing the spin-weighted Berry curvature: $D_{ab} = \int \frac{d\boldsymbol{k}}{8\pi^3} f_n (\Omega_a)_n (s_b)_n$ and f_n is the Fermi distribution function in terms of the original band spectrum ε_n. This result can be easily implemented in first-principles codes.

Equation (10) is one of the main results in this work. Strikingly, the response coefficient involves only a rank-2 tensor D_{ab}, in sharp contrast to the rank-3 pseudotensor in previous literatures [13–15]. To confirm its validity, we also use the linear response theory to derive the charge current and obtain the same result [40]. Moreover, since the relaxation time is not involved, Eq. (10) is the intrinsic contribution to the charge current. Experimentally, we expect a scaling law analysis for the longitudinal spin conductivity to confirm our theory.

The spin current in response to the electric field can also be calculated, by evaluating the local spin current operator $\boldsymbol{J}_S^0$ and the spin torque dipole $\boldsymbol{P}^T$ in either the semiclassical theory or the linear response theory. Since the derivation is standard, we leave it in the Supplemental Material [40]. The result reads as

$$\sigma'_{ijk} = \epsilon_{ika} D_{aj}. \tag{11}$$

Equations (10) and (11) together confirm the Onsager's reciprocal relation given in Eq. (6) for the intrinsic contribution. To see this, we first observe that from the expression of D_{ab}, the intrinsic contribution to the spin conductivity is even under time-reversal operation and hence even with respect to the magnetic order. Then the Onsager's reciprocal relation in Eq. (6) reduces to $\sigma_{ijk} = -\sigma'_{jki}$, which agrees with Eqs. (10) and (11).

Such Onsager's reciprocal relation has an important consequence: the intrinsic contribution to the spin conductivity does not dissipate heat. To see this, we consider the power generation of the spin transport: $P = \sigma_{ijk} E_i \partial_j B_k + \sigma'_{ijk} \partial_i B_j E_k$. Since the time-reversal-even part of the spin conductivity satisfies $\sigma_{ijk} = -\sigma'_{jki}$, we obtain $P = 0$. This again confirms the validity of our theory, as the intrinsic part does not contain any relaxation process and should not dissipate heat. Same property holds for the charge transport.

Due to the Levi-Civita symbol ϵ_{iaj}, the charge current is always normal to the spin current, i.e., only the Hall-type current exists for the intrinsic contribution. This is surprisingly similar to the intrinsic contribution to the anomalous Hall current: $(s_b)_n$ serves as the "charge" of the driving force and by replacing it with the electric charge $-e$, Eq. (10) reduces to the familiar Berry-phase contribution to the anomalous Hall conductivity. The geometrical origin of the inverse spin Hall effect is then the interplay of the "charge" and Berry curvature.

Since for the "charge" $(s_b)_n$ is a vector, it is natural to find that there are two types of Hall currents, depending on the relative orientation between the charge and the Hall-deflection plane. When $(\boldsymbol{s})_n$ is normal to the Hall-deflection plane (diagonal part of D_{ab}), we get the conventional inverse spin Hall effect; when $(\boldsymbol{s})_n$ is within the Hall-deflection plane

(off-diagonal part of D_{ab}), we obtain the planar inverse spin Hall effect. The latter one is our focus in this work.

To prove such classification, we note that as a rank-2 tensor, D_{ab} can always be split into a symmetric and antisymmetric part: $D^{s,as} = (D \pm D^T)/2$. Since D^s is orthogonal, it can always be diagonalized. Therefore, we can choose the real-space axis to be along the eigenvectors of D^s, imposing such diagonalization of D^s. The resulting charge and spin current reads as

$$J_i^{tr} = -\epsilon_{iaj} D^s_{aa} \partial_j B_a, \tag{12}$$

for a Zeeman field pointing along ath direction and changing along jth direction. We find that the spin polarization and flow direction of the spin current and the charge current flow direction are perpendicular to each other. This is thus the conventional spin Hall effect and its inverse, as shown in Fig. 1(a).

On the other hand, the antisymmetric part D^{as} always induces a charge current with the planar configuration, i.e., the PSHE and its inverse. To see this, we define a vector $\boldsymbol{d}$ from D^{as}:

$$\boldsymbol{d} = \frac{1}{2}\epsilon_{abc}\hat{e}_a D^{as}_{bc} = \int \frac{d\boldsymbol{k}}{16\pi^3} f_n \boldsymbol{\Omega}_n \times \boldsymbol{s}_n. \tag{13}$$

Due to the cross product, $\boldsymbol{d}$ is always perpendicular to spin and we thus refer to it as the spin-repulsion vector, which plays an essential role in the planar configuration of the current.

In terms of the spin-repulsion vector $\boldsymbol{d}$, the charge current reads as $J_i^{tr} = J_i^{\text{lon}} + J_i^{\text{tran}}$ with

$$J_i^{\text{lon}} = -d_i \partial_j B_j, \quad J_i^{\text{trans}} = d_j \partial_j B_i, \tag{14}$$

where $i \neq j$. Compared with the conventional inverse spin Hall effect in Eq. (12), only two different spatial indices appear, indicating a planar configuration. Moreover, the spin-repulsion vector can be either parallel with or perpendicular to the charge current flow, corresponding to the longitudinal and transverse configuration, respectively, as shown in Figs. 1(e) and 1(f).

We can also write the electric-field-induced spin current: $J_i^{s_j,\text{trans}} = d_i E_j$, $J_i^{s_i,\text{lon}} = -d_j E_j$, with $i \neq j$, as shown in Figs. 1(b) and 1(c). One immediately finds that the longitudinal PSHE supports a spin current with parallel spin polarization and flow direction. It can then be used for magnetization reversal of magnetic heterostructures with perpendicular magnetic anisotropy.

Finally, we comment that the above result only holds for nondegenerate bands. If the nth band is ℓ-fold degenerate, both s_b and Ω_a are $\ell \times \ell$ matrices. In this case, we find that the spin-weighted Berry curvature has the form $D_{ab} = \int \frac{d\boldsymbol{k}}{8\pi^3} f_n \text{Tr}(\Omega_a s_b)$ [40], which is gauge invariant under any SU(ℓ) rotation in the degenerate Hilbert space. Discussions based on nondegenerate D_{ab} can then be generated straightforwardly.

Symmetry requirement. Although the conventional and planar spin Hall effect share similar physical pictures, the study of the latter one only starts recently, due to its stringent symmetry requirements compared with the former one. Since both $\boldsymbol{s}$ and $\boldsymbol{\Omega}$ transform as an axial vector, the diagonal part D_{aa} is not subject to any symmetry constraint, consistent with the wide existence of the conventional spin Hall effect.

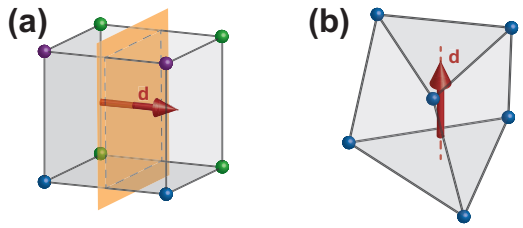

FIG. 2. The spin-repulsion vector in lattices with mirror symmetry (a) and rotational symmetry (b).

In contrast, to allow the PSHE, the spin-repulsion vector $\boldsymbol{d}$ must exist. Since $\boldsymbol{d}$ transforms as an axial vector under point-group operations, it flips sign under mirror operations that contain $\boldsymbol{d}$, but stays the same if the mirror plane is perpendicular to it; it also changes its direction under rotation about an axis perpendicular to it.

Based on this analysis, we find that among the 32 crystalline point groups, 13 of them allow an axial vector, including C_n, C_{nh} with $n = 1, 2, 3, 4, 6$, and S_{2n} with $n = 1, 2, 3$. In particular, $\boldsymbol{d}$ is perpendicular to the plane of the mirror symmetry and parallel with the rotational axis of C_n, as shown in Fig. 2.

The only experimental clue for the PSHE up to now is the mirror symmetry, which can be well explained by our theory. As a first example, we consider $MoTe_2$ [2]. The structure of the $MoTe_2$ film preserves only a single mirror symmetry with the mirror plane perpendicular to the interface. As a result, a spin-repulsion vector $\boldsymbol{d}$ parallel to the interface exists. Based on Fig. 1(b), when the electric field is applied parallel to $\boldsymbol{d}$, a spin current can flow out of the interface, with a spin magnetization also perpendicular to the interface, as observed in the experiment.

There are also magnetic materials allowing the PSHE. In our theory, $\boldsymbol{d}$ and magnetism can indeed coexist. However, as an axial vector, $\boldsymbol{d}$ is distinct from its fellow quantities, such as spin or magnetic field, in that $\boldsymbol{d}$ stays the same under time-reversal operation while spin and magnetic field flip sign. This has profound implications in magnetic materials. For example, in a ferromagnet with the magnetic point group $m'm'm$, the magnetization $\boldsymbol{M}$ is a natural axial vector, which lowers the symmetry of the crystal by breaking any mirror symmetry that contains $\boldsymbol{M}$. Nevertheless, $\boldsymbol{M}$ alone cannot support a nonzero $\boldsymbol{d}$ parallel to it: under the combined operation $\mathcal{M}T$ with any mirror plane containing $\boldsymbol{M}$, $\boldsymbol{M}$ stays the same but $\boldsymbol{d}$ flips sign. This difference excludes a simple ferromagnet as a candidate for the PSHE, unless the additional $\mathcal{M}T$ symmetry is further broken. It means that the intrinsic PSHE cannot be used to explain the current-induced s_z which changes its sign when the magnetization flips the direction, e.g., in Co and $MnAu_2$ [10,11].

We then identify all magnetic point groups that allow $\boldsymbol{d}$ as shown in Table I. Interestingly, $\boldsymbol{d}$ can exist in both ferromagnets and antiferromagnets. However, as discussed previously, since $\mathcal{M}T$ is equivalent to $\mathcal{M}$ for $\boldsymbol{d}$, only a single mirror operation may exist in all those groups, which are all perpendicular to the possible rotational axis.

Armed with this knowledge, we can offer unique perspectives to existing magnetic systems showing PSHE. A good

TABLE I. Magnetic point groups that allow the existence of $\boldsymbol{d}$, with the corresponding magnetic orders (F or AF). Magnetic point groups that explicitly contain the time-reversal symmetry are excluded as they have been discussed in the main text. Rhombic and cubic crystal systems forbid $\boldsymbol{d}$ and are hence not listed.

Crystal systems	Magnetic order	Group notation
Triclinic	F	$1, -1$
	AF	$-1'$
Monoclinic	F	$m, m', 2, 2', 2/m, 2'/m'$
	AF	$2/m', 2'/m$
Tetragonal	F	$4, 4/\mathrm{m}, -4$
	AF	$4', 4'/\mathrm{m}, 4/\mathrm{m}', 4'/\mathrm{m}', -4'$
Rhombohedral	F	$3, -3$
	AF	$-3'$
Hexagonal	F	$6, 6/\mathrm{m}, -6$
	AF	$6', 6'/\mathrm{m}, 6/\mathrm{m}', 6'/\mathrm{m}', -6'$

example is the Mn_3GaN film with the (001) plane as the interface [6]. Although the crystal symmetry is high, with both a fourfold-rotational symmetry and four mirror planes that contain the rotational axis, the antiferromagnetic order efficiently reduces the point-group symmetry without introducing any additional combined symmetry as discussed previously. The remaining mirror symmetry then allows $\boldsymbol{d}$ parallel to the interface, similar to $MoTe_2$, and the PSHE then emerges.

Both $MoTe_2$ and Mn_3GaN rely on the interface to lower the point-group symmetry of the bulk. In comparison, the collinear antiferromagnetic IrMn allows $\boldsymbol{d}$ in the single-crystal form. IrMn is a cubic crystal, and the antiferromagnetic ordering lowers the point-group symmetry to $2/m1'$. $\boldsymbol{d}$ is therefore allowed along the $[\bar{1}10]$ direction.

Special attention should be paid to the noncollinear antiferromagnet Mn_3Ir. The magnetic order lowers the crystal point-group symmetry to $-3m'$. Since the rotational axis is contained in the mirror plane, $\boldsymbol{d}$ is not allowed in such a system. Therefore, no intrinsic PSHE can exist in the bulk, contrary to the first-principle calculations [9,44]. This discrepancy may arise from the fact that the incomplete spin current operator is used in the DFT calculations and it points the currently observed spin accumulation with spin direction perpendicular to the interface to other origins [9], such as the magnetoelectric effect or heterostructures with special interfaces.

As discussed above, material systems based on the mirror symmetry can generally be explained by our theory. However, based on our symmetry analysis, we find that the spin-repulsion vector $\boldsymbol{d}$ and the PSHE consistent with the rotational symmetry are largely unexplored. This points alternative direction for future study of the PSHE. Candidates include Al_2CdS_4 (point group -4), VAu_4 (point group $4/m$), and BiI_3 (point group -3). Using VAu_4 as an example, we perform first-principle calculations of the planar spin Hall effect [40], and the result is consistent with the macroscopic symmetry analysis, showing the prediction potential of our theory.

The microscopic origin of the PSHE consistent with the rotational symmetry can be further illuminated. It is well established that the key element for spin Hall effect is the spin-orbital coupling, which is highly sensitive to the point-group symmetry. In crystals with the rotational symmetry, a minimal model for the conduction electron with a symmetry-allowed spin-orbital coupling can be put in the following form:

$$\hat{H} = \frac{k^2}{2m} + \lambda(k_x\sigma_y - k_y\sigma_x + k_z\sigma_z), \tag{15}$$

where the first term is the kinetic energy and the remaining terms are the spin-orbital coupling in three dimensions with $\boldsymbol{\sigma}$ being the Pauli matrix for spin. Such a model is chiral and respects the rotational symmetry about the z axis [45].

For a general chemical potential μ, the spin repulsion vector at zero temperature can be evaluated. The result reads as $\boldsymbol{d} = (0, 0, d_0)$ with (we take e, $\hbar$, and lattice constant a to be unity)

$$d_0 = \frac{\sqrt{2m\mu + m^2\lambda^2}}{6\pi^2}. \tag{16}$$

This is consistent with the symmetry analysis and the resulting PSHE increases with the chemical potential, as it is a Fermi-sea effect. The model in Eq. (15) then illustrates the type of spin-orbital coupling needed for the PSHE with rotational symmetry.

Discussions. We have shown that the intrinsic part of the spin conductivity is of rank 2 and the resulting PSHE is determined by a single polar vector $\boldsymbol{d}$. We shall note that the extrinsic contribution to the spin conductivity has been ignored, which may play an important role in some circumstances. For example, it has been known that, under the relaxation time approximation, for the previously studied rank-3 spin conductivity, its extrinsic part can yield a nonzero spin Hall effect in systems that satisfy different symmetry requirements as the intrinsic part [46,47].

Beyond the relaxation time approximation, the spin conductivity can be modified by the skew scattering and side jump contributions [15]. Although the skew scattering contribution is typically of higher order in different scattering times, the side jump contribution is proven to be independent of the disorder density and determined by the form of the scattering potential alone, hence usually being mixed with the intrinsic contribution. For example, it has been shown that for some special scattering potential, the side jump contribution can partially cancel the intrinsic part of the rank-3 spin conductivity [48,49], or fully cancel it to yield zero contribution at τ^0 [49]. In either case, our work offers a fresh start from a rank-2 intrinsic spin conductivity for future systematic study of the spin transport.

Acknowledgments. Y.G. acknowledges discussions with C. Xiao. Z.L. acknowledges the guidance from Z. Qiao. H.P., D.H., and Y.G. are supported by the National Key R&D Program (Grant No. 2022YFA1403502), Fundamental Research Funds for the Central Universities (Grant No. WK2340000102), and the National Natural Science Foundation of China (Grant No. 12234017). Y.G. is also supported by the Innovation Program for Quantum Science and Technology (Grant No. 2021ZD0302802). Z.L. is supported by Fundamental Research Funds for the Central Universities (Grants No. WK3510000010 and No. WK2030020032), the National Natural Science Foundation of China (Grants No. 11974327 and No. 12004369). Q.N. is supported by the National Natural

Science Foundation of China (Grant No. 12234017). We also thank the Supercomputing Center of University of Science and Technology of China for providing the high performance computing resources.

[1] J. E. Hirsch, Spin Hall effect, Phys. Rev. Lett. **83**, 1834 (1999).
[2] P. Song, C. H. Hsu, G. Vignale, M. Zhao, J. Liu, Y. Deng, W. Fu, Y. Liu, Y. Zhang, H. Lin, V. M. Pereira, and K. P. Loh, Coexistence of large conventional and planar spin Hall effect with long spin diffusion length in a low-symmetry semimetal at room temperature, Nat. Mater. **19**, 292 (2020).
[3] Q. Xie, W. Lin, S. Sarkar, X. Shu, S. Chen, L. Liu, T. Zhao, C. Zhou, H. Wang, J. Zhou, S. Gradecak, and J. Chen, Field-free magnetization switching induced by the unconventional spin-orbit torque from WTe_2, APL Mater. **9**, 051114 (2021).
[4] L. Liu, O. J. Lee, T. J. Gudmundsen, D. C. Ralph, and R. A. Buhrman, Current-induced switching of perpendicularly magnetized magnetic layers using spin torque from the spin Hall effect, Phys. Rev. Lett. **109**, 096602 (2012).
[5] D. MacNeill, G. M. Stiehl, M. H. D. Guimaraes, R. A. Buhrman, J. Park, and D. C. Ralph, Control of spin-orbit torques through crystal symmetry in WTe_2/ferromagnet bilayers, Nat. Phys. **13**, 300 (2017).
[6] T. Nan, C. X. Quintela, J. Irwin, G. Gurung, D. F. Shao, J. Gibbons, N. Campbell, K. Song, S. Y. Choi, L. Guo, R. D. Johnson, P. Manuel, R. V. Chopdekar, I. Hallsteinsen, T. Tybell, P. J. Ryan, J. W. Kim, Y. Choi, P. G. Radaelli, D. C. Ralph *et al.*, Controlling spin current polarization through non-collinear antiferromagnetism, Nat. Commun. **11**, 4671 (2020).
[7] L. Liu, C. Zhou, X. Shu, C. Li, T. Zhao, W. Lin, J. Deng, Q. Xie, S. Chen, J. Zhou, R. Guo, H. Wang, J. Yu, S. Shi, P. Yang, S. Pennycook, A. Manchon, and J. Chen, Symmetry-dependent field-free switching of perpendicular magnetization, Nat. Nanotechnol. **16**, 277 (2021).
[8] J. Zhou, X. Shu, Y. Liu, X. Wang, W. Lin, S. Chen, L. Liu, Q. Xie, T. Hong, P. Yang, B. Yan, X. Han, and J. Chen, Magnetic asymmetry induced anomalous spin-orbit torque in IrMn, Phys. Rev. B **101**, 184403 (2020).
[9] Y. Liu, Y. Liu, M. Chen, S. Srivastava, P. He, K. L. Teo, T. Phung, S. H. Yang, and H. Yang, Current-induced out-of-plane spin accumulation on the (001) surface of the $IrMn_3$ antiferromagnet, Phys. Rev. Appl. **12**, 064046 (2019).
[10] T. C. Chuang, D. Qu, S. Y. Huang, and S. F. Lee, Magnetization-dependent spin Hall effect in a perpendicular magnetized film, Phys. Rev. Res. **2**, 032053(R) (2020).
[11] X. Chen, S. Shi, G. Shi, X. Fan, C. Song, X. Zhou, H. Bai, L. Liao, Y. Zhou, H. Zhang, A. Li, Y. Chen, X. Han, S. Jiang, Z. Zhu, H. Wu, X. Wang, D. Xue, H. Yang, and F. Pan, Observation of the antiferromagnetic spin Hall effect, Nat. Mater. **20**, 800 (2021).
[12] R. Galceran, B. Tian, J. Li, F. Bonell, M. Jamet, C. Vergnaud, A. Marty, J. H. García, J. F. Sierra, M. V. Costache, S. Roche, S. O. Valenzuela, A. Manchon, X. Zhang, and U. Schwingenschlögl, Control of spin-charge conversion in van der Waals heterostructures, APL Mater. **9**, 100901 (2021).
[13] J. Sinova, D. Culcer, Q. Niu, N. A. Sinitsyn, T. Jungwirth, and A. H. MacDonald, Universal intrinsic spin Hall effect, Phys. Rev. Lett. **92**, 126603 (2004).
[14] M. Gradhand, D. V. Fedorov, F. Pientka, P. Zahn, I. Mertig, and B. L. Györffy, First-principle calculations of the berry curvature of bloch states for charge and spin transport of electrons, J. Phys.: Condens. Matter **24**, 213202 (2012).
[15] J. Sinova, S. O. Valenzuela, J. Wunderlich, C. H. Back, and T. Jungwirth, Spin Hall effects, Rev. Mod. Phys. **87**, 1213 (2015).
[16] M. Seemann, D. Ködderitzsch, S. Wimmer, and H. Ebert, Symmetry-imposed shape of linear response tensors, Phys. Rev. B **92**, 155138 (2015).
[17] Q. F. Sun, X. C. Xie, and J. Wang, Persistent spin current in nanodevices and definition of the spin current, Phys. Rev. B **77**, 035327 (2008).
[18] R. S. Akzyanov and A. L. Rakhmanov, Bulk and surface spin conductivity in topological insulators with hexagonal warping, Phys. Rev. B **99**, 045436 (2019).
[19] C. Xiao and Q. Niu, Unified bulk semiclassical theory for intrinsic thermal transport and magnetization currents, Phys. Rev. B **101**, 235430 (2020).
[20] A. Roy, M. H. D. Guimarães, and J. Sławińska, Unconventional spin Hall effects in nonmagnetic solids, Phys. Rev. Mater. **6**, 045004 (2022).
[21] Y. Zhang, Q. Xu, K. Koepernik, R. Rezaev, O. Janson, J. Železný, T. Jungwirth, C. Felser, J. van den Brink, and Y. Sun, Different types of spin currents in the comprehensive materials database of nonmagnetic spin Hall effect, npj Comput. Mater. **7**, 167 (2021).
[22] J. H. Cullen, P. Bhalla, E. Marcellina, A. R. Hamilton, and D. Culcer, Generating a topological anomalous Hall effect in a nonmagnetic conductor: An in-plane magnetic field as a direct probe of the berry curvature, Phys. Rev. Lett. **126**, 256601 (2021).
[23] R. B. Atencia, Q. Niu, and D. Culcer, Semiclassical response of disordered conductors: Extrinsic carrier velocity and spin and field-corrected collision integral, Phys. Rev. Res. **4**, 013001 (2022).
[24] D. Culcer, J. Sinova, N. A. Sinitsyn, T. Jungwirth, A. H. MacDonald, and Q. Niu, Semiclassical spin transport in spin-orbit-coupled bands, Phys. Rev. Lett. **93**, 046602 (2004).
[25] Q. F. Sun and X. C. Xie, Definition of the spin current: The angular spin current and its physical consequences, Phys. Rev. B **72**, 245305 (2005).
[26] J. Shi, P. Zhang, D. Xiao, and Q. Niu, Proper definition of spin current in spin-orbit coupled systems, Phys. Rev. Lett. **96**, 076604 (2006).
[27] N. Nagaosa, Spin currents in semiconductors, metals, and insulators, J. Phys. Soc. Jpn. **77**, 031010 (2008).
[28] N. Sugimoto, S. Onoda, S. Murakami, and N. Nagaosa, Spin Hall effect of a conserved current: Conditions for a nonzero spin Hall current, Phys. Rev. B **73**, 113305 (2006).
[29] T. W. Chen, C. M. Huang, and G. Y. Guo, Conserved spin and orbital angular momentum Hall current in a two-dimensional electron system with Rashba and Dresselhaus spin-orbit coupling, Phys. Rev. B **73**, 235309 (2006).
[30] P. Zhang, Z. Wang, J. Shi, D. Xiao, and Q. Niu, Theory of conserved spin current and its application to a two-dimensional hole gas, Phys. Rev. B **77**, 075304 (2008).

[31] T. W. Chen and G. Y. Guo, Torque and conventional spin Hall currents in two-dimensional spin-orbit coupled systems: Universal relation and hyperselection rule, Phys. Rev. B **79**, 125301 (2009).

[32] G. Liu, P. Zhang, Z. Wang, and S. S. Li, Spin Hall effect on the kagome lattice with Rashba spin-orbit interaction, Phys. Rev. B **79**, 035323 (2009).

[33] A. Rückriegel and P. Kopietz, Spin currents, spin torques, and the concept of spin superfluidity, Phys. Rev. B **95**, 104436 (2017).

[34] R. J. H. Wesselink, K. Gupta, Z. Yuan, and P. J. Kelly, Calculating spin transport properties from first principles: Spin currents, Phys. Rev. B **99**, 144409 (2019).

[35] L. Dong, C. Xiao, B. Xiong, and Q. Niu, Berry phase effects in dipole density and the Mott relation, Phys. Rev. Lett. **124**, 066601 (2020).

[36] S. R. De Groot and P. Mazur, *Non-Equilibrium Thermodynamics* (Dover, New York, 1962).

[37] J. Jackson, *Classical Electrodynamics* (Wiley, New York, 1998).

[38] D. Xiao, M. C. Chang, and Q. Niu, Berry phase effects on electronic properties, Rev. Mod. Phys. **82**, 1959 (2010).

[39] Y. Zhao, Y. Gao, and D. Xiao, Electric polarization in inhomogeneous crystals, Phys. Rev. B **104**, 144203 (2021).

[40] See Supplemental Material at http://link.aps.org/supplemental/10.1103/PhysRevResearch.6.L012034 for discussions of the entropy production rate, the Onsager's reciprocal relation, the definition and physical meaning of the total spin current, the charge current in response to the Zeeman field gradient using the semiclassical and linear response theory, the total spin current in response to the electric field, the non-Abelian spin conductivity, the spin conductivity in a model system with time reversal and inversion symmetry, and first-principles calculation of the spin conductivity in VAu4.

[41] L. D. Landau and E. M. Lifshitz, *Statistical Physics* (Butterworth-Heinemann, Oxford, 1980).

[42] D. Xiao, Y. Yao, Z. Fang, and Q. Niu, Berry-phase effect in anomalous thermoelectric transport, Phys. Rev. Lett. **97**, 026603 (2006).

[43] Y. Gao, D. Vanderbilt, and D. Xiao, Microscopic theory of spin toroidization in periodic crystals, Phys. Rev. B **97**, 134423 (2018).

[44] Y. Zhang, Y. Sun, H. Yang, J. Železný, S. P. P. Parkin, C. Felser, and B. Yan, Strong anisotropic anomalous Hall effect and spin Hall effect in the chiral antiferromagnetic compounds Mn_3X (X = Ge, Sn, Ga, Ir, Rh, and Pt), Phys. Rev. B **95**, 075128 (2017).

[45] X. Q. Sun, S. C. Zhang, and Z. Wang, Helical spin order from topological Dirac and Weyl semimetals, Phys. Rev. Lett. **115**, 076802 (2015).

[46] R. González-Hernández, L. Šmejkal, K. Výborný, Y. Yahagi, J. Sinova, T. Jungwirth, and J. Železný, Efficient electrical spin splitter based on nonrelativistic collinear antiferromagnetism, Phys. Rev. Lett. **126**, 127701 (2021).

[47] A. Bose, N. J. Schreiber, R. Jain, D. F. Shao, H. P. Nair, J. Sun, X. S. Zhang, D. A. Muller, E. Y. Tsymbal, D. G. Schlom, and D. C. Ralph, Tilted spin current generated by the collinear antiferromagnet ruthenium dioxide, Nat. Electronics **5**, 267 (2022).

[48] C. Xiao and Q. Niu, Conserved current of nonconserved quantities, Phys. Rev. B **104**, L241411 (2021).

[49] R. Raimondi, P. Schwab, C. Gorini, and G. Vignale, Spin-orbit interaction in a two-dimensional electron gas: A $SU(2)$ formulation, Ann. Phys. (Berlin) **524**, 153162 (2012).